Original Article
Role of pre-*miR-532* (*miR-532-5p* and *miR-532-3p*) in regulation of gene expression and molecular pathogenesis in renal cell carcinoma

Yasutaka Yamada[1,2], Takayuki Arai[1,2], Mayuko Kato[1,2], Satoko Kojima[3], Shinichi Sakamoto[2], Akira Komiya[2], Yukio Naya[3], Tomohiko Ichikawa[2], Naohiko Seki[1]

Departments of [1]Functional Genomics, [2]Urology, Chiba University Graduate School of Medicine, Chiba, Japan; [3]Department of Urology, Teikyo University Chiba Medical Center, Ichihara, Japan

Abstract: Analyses of our previously determined microRNA (miRNA) expression signature of renal cell carcinoma (RCC) and The Cancer Genome Atlas (TCGA) database revealed that both strands of the pre-*miR-532-duplex-miR-532-5p* (the guide strand) and *miR-532-3p* (the passenger strand)- are closely associated with poor prognosis of RCC patients (P = 0.0411 and P = 0.022, respectively). In this study we investigated the functional significance of these miRNAs and identified gene targets involved in RCC pathogenesis. Ectopic expression of these miRNAs significantly attenuated the malignant phenotypes including proliferation, migration and invasion of two RCC cell lines, 786-O and A498. A combination of genome-wide gene expression and *in silico* database analyses revealed 36 and 34 genes as putative target oncogenes regulated by *miR-532-5p* and *miR-532-3p*, respectively, in RCC cells. Among these targets, expression of aquaporin9 (*AQP9*), a water channel protein, was directly regulated by both *miR-532-5p* and *miR-532-3p*, and high expression levels of *AQP9* were significantly associated with poor prognosis of RCC patients (P = 2.03e-05). Multivariate analysis indicated that *APQ9* expression is an independent prognostic factor for RCC patients. Aberrant AQP9 expression at both the gene and protein level was detected in RCC clinical specimens. siRNA-mediated knockdown *of AQP9* by si-*AQP9* inhibited the malignant phenotypes of RCC cells. Rescue assays of *AQP9* overexpression showed that the *miR-532/AQP9* axis was closely involved in RCC oncogenesis. The identification of antitumor miRNAs and their targets will contribute to an increased understanding of the molecular pathogenesis of RCC.

Keywords: microRNA, antitumor, *miR-532-5p*, *miR-532-3p*, passenger strand, renal cell carcinoma, *AQP9*

Introduction

Renal cell carcinoma (RCC) accounts for 2-3% of all adult cancers and is the seventh and ninth most common cancer for men and women, respectively [1]. An estimated 209,000 new cases and 102,000 deaths due to all RCCs occur annually worldwide [1]. There are many RCC types including clear cell RCC, papillary RCC, chromophobe RCC and collecting duct RCC. Each type of RCC has distinct characteristics and is derived from a different cell lineage. The most common type of RCC is clear cell RCC (ccRCC), that represents approximately 75%-85% of RCC [2].

The 5-year overall survival rate of patients with early-stage RCC is approximately 60%, where-as the rate for patients with metastasis or advanced-stage is far lower, at less than 10% [1]. Between 30% and 40% of patients with early-stage RCC develop local recurrence or distant metastasis [2]. Several recently developed treatment strategies for RCC, such as mTOR-targeted agents, VEGF-tyrosine kinase inhibitors and immune checkpoint inhibitors, have slightly improved overall survival rates for patients with metastatic disease [3]. Despite these improvements, the 5-year survival of advanced RCC continues to be around 20% [3]. Elucidation of metastatic pathways and therapeutic targets will be essential for achieving improved outcomes for RCC patients.

Advanced cancer-genome technologies have highlighted the important role that noncoding

Table 1. Characteristics of 23 patients with non-metastatic clear cell RCC

No.	Age at operation	Sex	Tumor Grade	pT	remarks
1	71	F	G2	T1a	qRT-PCR
2	74	M	G1>G2	T1a	qRT-PCR
3	59	M	G3>G2	T1b	qRT-PCR
4	52	M	G2>G3>G1	T1a	qRT-PCR
5	64	M	G2>G3	T1b	qRT-PCR
6	67	M	G2>G3>G1	T3a	qRT-PCR
7	59	M	G3	T3a	qRT-PCR
8	61	M	G2>G1	T1a	qRT-PCR
9	73	M	G1>>G3	T2a	qRT-PCR
10	77	M	G1>G2	T1b	qRT-PCR
11	77	M	G2>G1	T3a	qRT-PCR
12	66	M	G2>G1	T1a	qRT-PCR
13	51	F	G2>G1>G3	T3a	qRT-PCR
14	47	M	G2>G1	T1b	qRT-PCR
15	78	M	G2>G1>>G3	T1b	qRT-PCR
16	44	M	G2>G1	T1a	qRT-PCR
17	57	M	G1>G2	T1a	qRT-PCR
18	54	M	G2>G1	T3a	qRT-PCR
19	72	F	G1>>G2	T1b	qRT-PCR
20	70	M	G3>G2	T3a	qRT-PCR
21	71	M	G2>G1	T1a	IHC
22	66	F	G2	T1b	IHC
23	68	M	G1	T1b	IHC

RCC, renal cell carcinoma; F, female; M, male; qRT-PCR, quantitative reverse transcription polymerase chain reaction; IHC, immunohistochemistry.

RNAs play in disease pathogenesis. Noncoding, single-stranded microRNAs (miRNAs) have 19 to 22 nucleotides and can fine-tune expression of both protein coding and non-coding genes by repressing translation or cleaving RNA transcripts in a sequence-dependent manner [4]. A single miRNA can regulate a large number of protein-coding and noncoding RNA transcripts in relevant cells. As such, aberrant expression of miRNAs can have broad-ranging effects on RNA networks within cells. Numerous studies have revealed that dysregulated miRNA expression can disrupt tightly controlled RNA networks. Such disruptions are closely related to cancer cell development, metastasis and drug resistance [4].

Based on miRNA expression signatures in RCC, we sequentially identified antitumor miRNAs and the oncogenic targets they directly control, including *miR-101* (target *UHRF1*), *miR-10a-5p* (*SKA1*), *miR-26a/miR-26b* (*LOXL2* and *PLOD2*) and *miR-451a* (*PMM2*) [5-8]. We recently showed that both strands of the pre-miRNAs pre-*miR-144* and pre-*miR-455* acted as antitumor miRNAs in RCC cells and the oncogenic genes they target are closely involved in RCC pathogenesis [9, 10]. The conventional theory for the biological function of miRNA suggested that the guide strands of miRNA can control expression of target genes, whereas passenger strands are degraded and have no function [11]. However, our studies revealed that several miRNA passenger strands can indeed regulate target gene expression and the aberrant expression of these miRNAs is involved in RCC oncogenesis.

Analyses of our original miRNA expression signature for RCC and The Cancer Genome Atlas (TCGA) database revealed that both *miR-532-5p* (the guide strand) and *miR-532-3p* (the passenger strand) are closely associated with poor prognosis of RCC patients ($P = 0.0411$ and $P = 0.022$, respectively). Here we investigated the functional significance of these miRNAs in terms of the oncogenes they target and their role in RCC pathogenesis.

Materials and methods

Clinical RCC specimens and RCC cell lines

A total of 23 clinical RCC tissue samples were obtained from patients that underwent total nephrectomy at Chiba University Hospital between 2008 and 2015 (**Table 1**). No patient had metastatic sites at the time of surgery. All patients in this study signed informed consent and the present study protocol was approved by the Institutional Review Board of Chiba University (acceptance number: 484). We used the RCC cell lines 786-O and A498 that were obtained from the American Type Culture Collection (ATCC, Manassas, VA, USA).

Transfection of mature miRNA, siRNA or plasmid vectors

We used the following RNAs in this study: pre-miR miRNA precursors (*hsa-miR-532-5p*, assay ID: PM11553; *hsa-miR-532-3p*, assay ID: PM12824; Applied Biosystems, Foster City, CA, USA), negative control miRNA (assay ID: AM

17111; Applied Biosystems) and siRNA (Stealth Select RNAi siRNA; si-*AQP9,* P/N: HSS-100615 and HSS100617; Invitrogen, Carlsbad, CA, USA). The *AQP9* plasmid vector was provided by ORIGENE (cat. no. SC113060; Rockville, MD, USA). Transfections were carried out using previously described procedures [8]. miRNAs and siRNAs were incubated with Opti-MEM (Invitrogen) and Lipofectamine RNAi Max transfection reagent at 10 nM (Invitrogen). Plasmid vectors were incubated with Opti-MEM and Lipofectamine 3000 reagent (Invitrogen) for forward transfection.

Quantitative real-time reverse transcription polymerase chain reaction (qRT-PCR)

TaqMan probes and *AQP9* primers (P/N: Hs01033361_m1; Applied Biosystems) were assay-on-demand gene expression products. qRT-PCR for *miR-532-5p* (P/N: 001518; Applied Biosystems) and *miR-532-3p* (P/N: 002355; Applied Biosystems) was used to validate miRNA expression. To normalize the data for analysis of mRNAs and miRNAs, *GUSB* (P/N: Hs-99999908_m1; Applied Biosystems) and *RNU48* (assay ID: 001006; Applied Biosystems) were used. PCR quantification was carried out as described previously [12].

Cell proliferation, migration, and invasion assays

Cell proliferation activity was determined using the XTT assay with the Cell Proliferation Kit II (Sigma-Aldrich, St. Louis, MO, USA). Cell migration was assessed using wound healing assays. Cell invasion activity was determined using modified Boyden chambers containing Matrigel-coated Transwell membrane filter inserts.

Western blotting

Western blotting was performed with polyclonal anti-AQP9 antibodies (1:200 dilution; SAB-4301752; Sigma-Aldrich). We used anti-glyceraldehyde 3-phosphate dehydrogenase (GAPDH) antibodies (1:10,000 dilution; ab8245; Abcam, Cambridge, UK) as a control.

Incorporation of miR-532-5p and miR-532-3p into the RISC by Ago2 immunoprecipitation

A498 cells were transfected with 10 nM miRNA by reverse transfection. After 72 h, immunoprecipitation was performed using an Ago2 miRNA

isolation kit (Wako, Osaka, Japan). Expression levels of *miR-532-5p* and *miR-532-3p* were analyzed by qRT-PCR. miRNA data were normalized to *miR-26a* expression (P/N: 000405; Applied Biosystems), which was not affected by *miR-532-5p* and *miR-532-3p*.

Identification of candidate target genes regulated by miR-532-5p and miR-532-3p

Candidate target genes regulated by *miR-532-5p* and *miR-532-3p* were identified using a combination of *in silico* and genome-wide gene expression analyses and listed in the TargetScan database (release 7.0) in a sequence-dependent manner (http://www.targetscan.org/vert_70/). Upregulated genes in RCC were identified from public data in the Gene Expression Omnibus (GEO; accession number: GSE36895) and we narrowed down the candidate genes. Gene expression was analyzed with our own oligo microarray data analyses (Human GE 60K; Agilent Technologies) that were deposited into the GEO (on June 14th, 2018; http://www.ncbi.nlm.nih.gov/geo/) under accession number GSE115800.

Dual-luciferase reporter assay

The wild-type sequence of the *AQP9* 3'-UTR was inserted between the *Sgf*I and *Pme*I restriction sites in the 3'-UTR of the hRluc gene in the psiCHECK-2 vector (C8021; Promega, Madison, WI, USA). We used sequences that were deleted in the *miR-532-5p* (position 1604-1610) and *miR-532-3p* (position 935-941) target sites. psiCHECK-2 vector was used as a cloning vector for the synthesized DNA [8].

Immunohistochemistry

Immunohistochemistry procedures were performed according to a previously described method [12]. Clinical tissue sections were incubated overnight at 4°C with anti-AQP9 antibodies diluted 1:20 (SAB4301752; Sigma-Aldrich).

Analysis of genes downstream of AQP9

To investigate *AQP9*-regulated pathways in RCC cells we assessed gene expression changes in A498 cells transfected with si-*AQP9*. Microarray data were used for expression profiling of si-*AQP9* transfectants. The data were deposited into the GEO on December 4, 2018 (accession number: GSE123317).
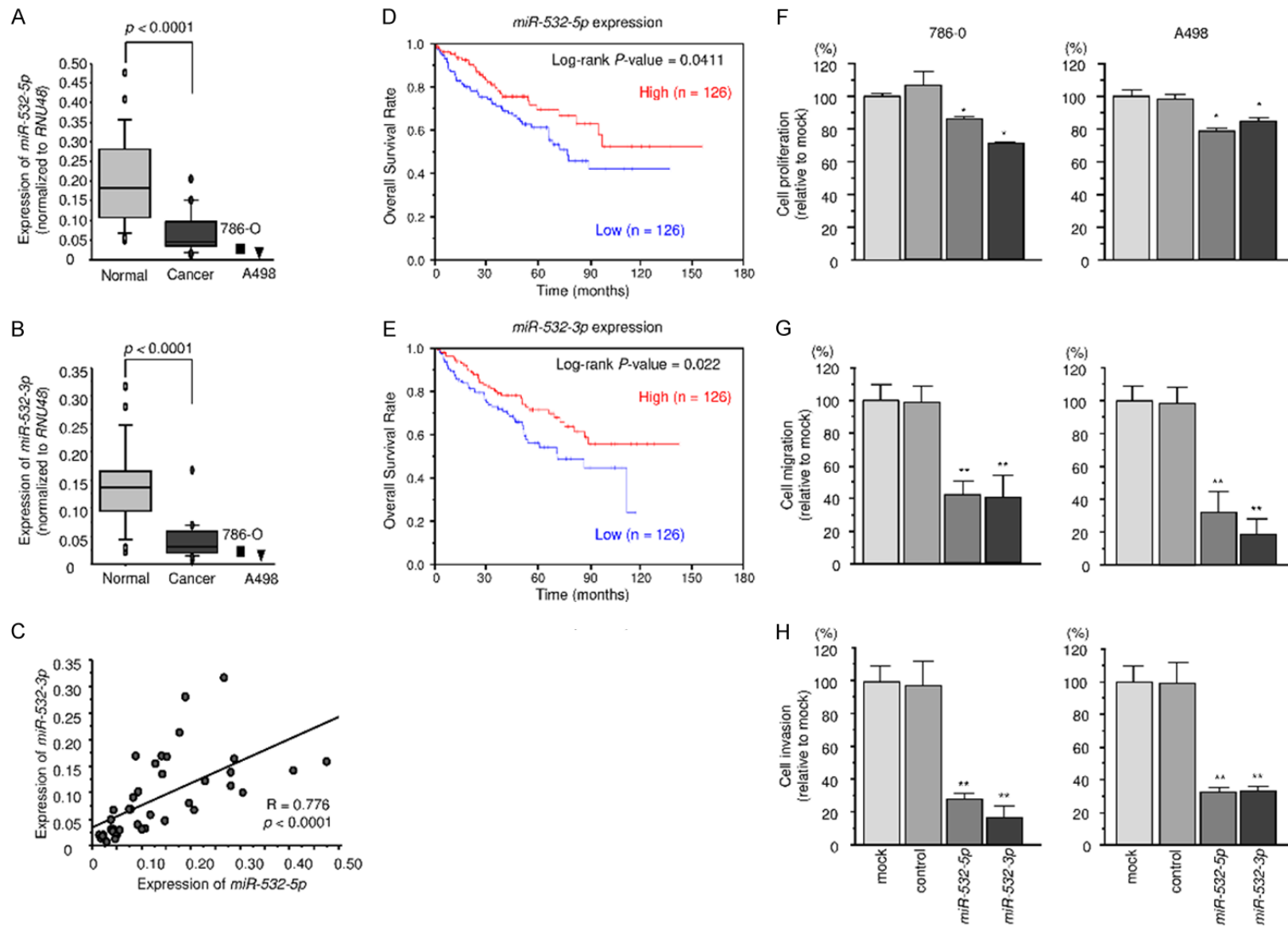
Figure 1. *miR-532-duplex* expression, relation to prognosis, and function. A-C. Expression levels of *miR-532-5p* and *miR-532-3p* in RCC clinical specimens. *RNU48* was used as an internal control. Expression levels of *miR-532-5p* and *miR-532-3p* were positively correlated by Spearman's rank test. D, E. Based on TCGA database, low expression levels of both *miR-532-5p* and *miR-532-3p* were significantly associated with poor prognosis. F-H. Cell proliferation, migration and invasion activities. $^{*}P < 0.01$, $^{**}P < 0.0001$.
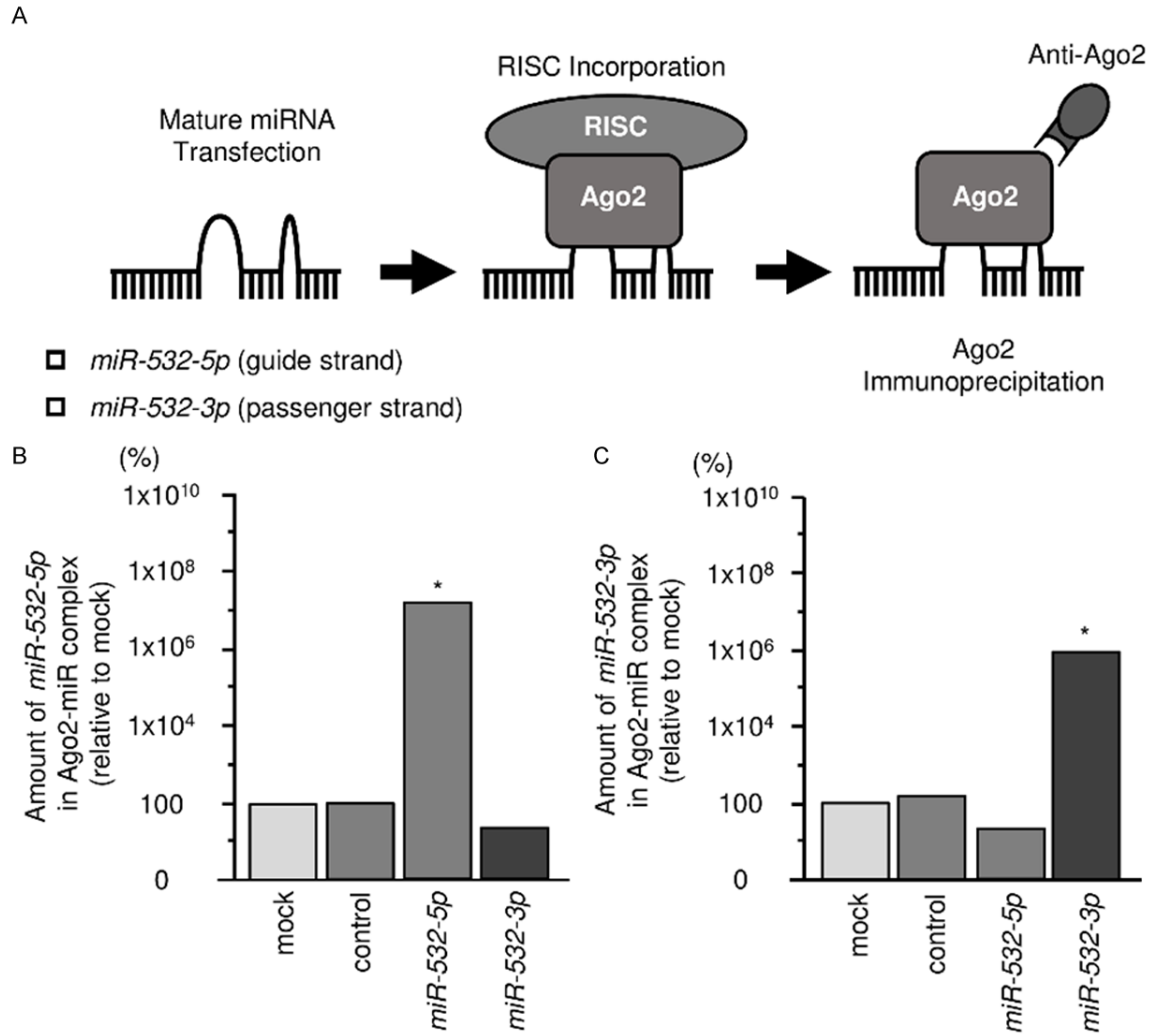
Figure 2. Incorporation of *miR-532-5p* and *miR-532-3p* into the RISC. A. Schematic diagram illustrating Ago2 immunoprecipitation. B, C. Amount of *miR-532-5p* and *miR-532-3p* in Ago2 immunoprecipitates of cell lysates from cells transfected transfection with *miR-532-5p* or *miR-532-3p*. The amount shown is relative to mock-transfected cells. $^*P < 0.0001$.

Analysis of clinical significance of the miR-532-duplex and AQP9

We examined the clinical importance of miR-NAs and genes in RCC patients using the RNA sequencing database in TCGA (https://tcga-data.nci.nih.gov/tcga/). The gene expression and clinical information were obtained from cBioportal (http://www. cbioportal.org/ and the provisional data were downloaded on September 1, 2018 [13-15].

Statistical analysis

Statistical analyses involving two or three variables and numerical values were analyzed by Bonferroni-adjusted Mann-Whitney U tests. Spearman's rank tests were used to analyze correlations between expression levels. Expert StatView software (version 5.0, SAS Institute Inc., Cary, NC, USA) was used for these analyses. Multivariate analysis with JMP Pro 13 was used to analyze prognostic factors for patient survival.

Results

Analysis of miR-532-5p and miR-532-3p expression levels in clinical tissue samples

In the human genome, *miR-532* is located on chromosome Xp11.23. The mature sequences
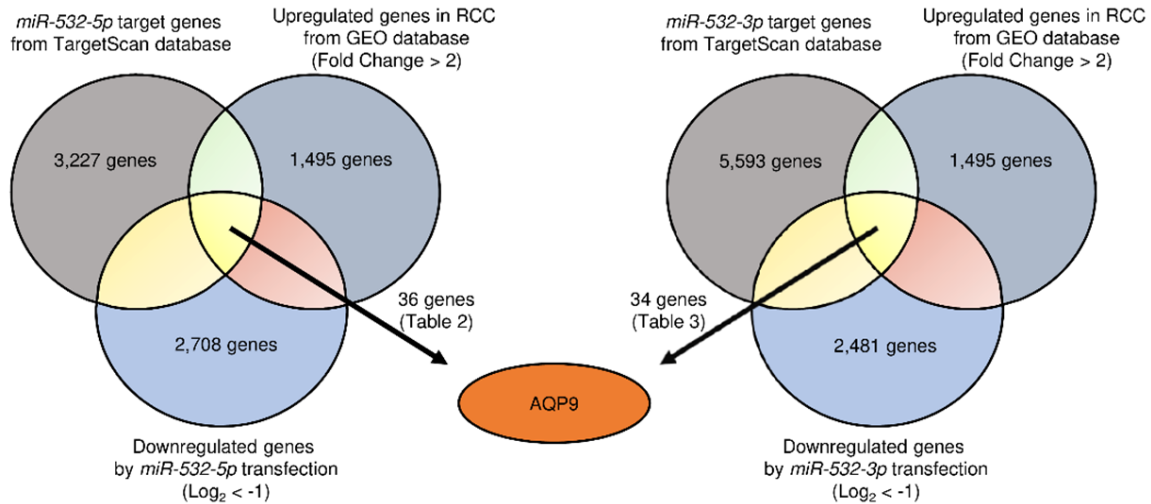
Figure 3. Search strategy to identify *miR-532-5p* and *miR-532-3p* target genes. The venn diagram represents genes identified through a search of the TargetScan database to identify genes carrying miR-532 binding sites as well as genes that have up- or down-regulated expression in the GEO database for RCC patients and in *miR-532*-transfected cells.

of *miR-532-5p* and *miR-532-3p* are 5'-CAUGC-CUUGAGUGUAGGACCGU-3' and 5'-CCUCCCA-CACCCAAGGCUUGCA-3', respectively. The expression levels of *miR-532-5p* and *miR-532-3p* were significantly decreased in cancer tissues compared with those in adjacent noncancerous tissues ($P < 0.0001$; **Figure 1A**, **1B**). In addition, Spearman's rank test showed a strong positive correlation between *miR-532-5p* and *miR-532-3p* expression levels in RCC specimens (R = 0.776, $P < 0.0001$; **Figure 1C**).

Clinical significance and functional analysis of miR-532-5p and miR-532-3p

From TCGA database, low expression levels of *miR-532-5p* and *miR-532-3p* were significantly associated with a shorter survival period for RCC patients ($P = 0.0411$ and $P = 0.022$, respectively, **Figure 1D, 1E**). In both 786-O and A498 cells, restoration of *miR-532-5p* and *miR-532-3p* expression indicated that both miRNAs could suppress cancer cell proliferation, migration and invasion activities (**Figure 1F-H**).

Incorporation of miR-532-5p and miR-532-3p into the RISC

We next performed immunoprecipitation with antibodies targeting Ago2, which plays a pivotal role in the uptake of miRNAs into the RNA-induced silencing complex (RISC) (**Figure 2A**). After transfection of A498 cells with *miR-532-5p* and immunoprecipitation by anti-Ago2 antibodies, *miR-532-5p* levels in the immunoprecipitates were significantly higher than those of mock- or miR-control-transfected cells and those of *miR-532-3p*-transefected cells ($P < 0.0001$; **Figure 2B**). Similarly, after *miR-532-3p* transfection, substantial amounts of *miR-532-3p* were detected in Ago2 immunoprecipitates ($P < 0.0001$; **Figure 2C**).

Identification of candidate target genes of miR-532-5p and miR-532-3p regulation

We next searched for genes that had putative target sites for *miR-532-5p* and *miR-532-3p* in their 3'-UTR and that showed upregulated expression levels (Fold Change > 2) in RCC tissues and downregulated expression in RCC cells transfected with *miR-532-5p* or *miR-532-3p* (Log$_2$ ratio < -1) (**Figure 3**). Using this search strategy, we identified 36 and 34 genes as candidate target genes of *miR-532-5p* and *miR-532-3p*, respectively (**Tables 2**, **3**). Among these candidate genes, RCC patients with high expression of 10 genes and 11 genes had significantly poor prognosis from TCGA database (**Figures 4**, **5**). We focused on aquaporin9 (*AQP9*), which is targeted by both *miR-532-5p* and *miR-532-3p*, because aquaporins affect not only water and small molecule permeability but are also implicated in the development of several types of cancers.

Table 2. Candidate *miR-532-5p* target genes in RCC

Gene Symbol	Gene Name	Entrez Gene ID	Cytoband	GEO expression data Fold-Change (Tumor/Normal)	*miR-532-5p* transfection in 786-O (Log$_2$ ratio)	Binding Sites Count	TCGA analysis for OS(high vs low expression: *p* value)
FAM64A	Family with sequence similarity 64N, member A	54478	hs|17p13.2	2.400	-1.450	1	1.79E-07
CEP55	Centrosomal protein 55kDa	55165	hs|10q23.33	4.202	-1.891	1	6.94E-07
AQP9	Aquaporin 9	366	hs|15q21.3	2.077	-1.470	1	2.03E-05
DEPDC1	DEP domain containing 1	55635	hs|1p31.2	2.607	-2.934	1	0.000111
TCF19	Transcription factor 19	6941	hs|6p21.33	3.277	-1.199	1	0.000554
MKI67	Antigen identified by monoclonal antibody Ki-67	4288	hs|10q26.2	2.039	-1.047	1	0.00106
PAQR4	Progestin and adipoQ receptor family member IV	124222	hs|16p13.3	5.134	-1.173	1	0.00152
CENPK	Centromere protein K	64105	hs|5q12.3	4.442	-1.556	1	0.00234
KIAA0101	KIAA0101	9768	hs|15q22.31	3.359	-1.237	2	0.00258
CSF1	Colony stimulating factor 1 (macrophage)	1435	hs|1p13.3	2.021	-1.547	0	0.027
KIAA1715	KIAA1715	80856	hs|2q31.1	2.170	-2.271	2	0.0592
BCAT1	Branched chain amino-acid transaminase 1, cytosolic	586	hs|12p12.1	3.076	-2.187	3	0.1
MEGF6	Multiple EGF-like-domains 6	1953	hs|1p36.32	2.113	-2.224	1	0.151
MCTP2	Multiple C2 domains, transmembrane 2	55784	hs|15q26.2	2.072	-1.484	2	0.191
NOTCH4	Notch 4	4855	hs|6p21.32	2.169	-1.025	1	0.21
RASSF5	Ras association (RalGDS/AF-6) domain family member 5	83593	hs|1q32.1	2.840	-2.636	2	0.273
SIPA1L2	Signal-induced proliferation-associated 1 like 2	57568	hs|1q42.2	2.462	-1.356	1	0.28
CHSY3	Chondroitin sulfate synthase 3	337876	hs|5q23.3	4.220	-1.391	1	0.318
ABCA12	ATP-binding cassette, sub-family A (ABC1), member 12	26154	hs|2q35	3.975	-3.277	1	0.32
PLK2	Polo-like kinase 2	10769	hs|5q11.2	5.045	-1.428	1	0.327
HHIPL1	HHIP-like 1	84439	hs|14q32.2	2.044	-1.318	1	0.343
LZTS1	Leucine zipper, putative tumor suppressor 1	11178	hs|8p21.3	2.138	-2.116	1	0.426
SLAMF7	SLAM family member 7	57823	hs|1q23.3	4.181	-2.447	2	0.44
ERO1L	ERO1-like (S. cerevisiae)	30001	hs|14q22.1	2.829	-2.441	0	0.444
NCF2	Neutrophil cytosolic factor 2	4688	hs|1q25.3	3.432	-2.254	1	0.495
GBP1	Guanylate binding protein 1, interferon-inducible	2633	hs|1p22.2	3.410	-3.062	1	0.523
ITGA4	Integrin, alpha 4 (antigen CD49D, alpha 4 subunit of VLA-4 receptor)	3676	hs|2q31.3	2.336	-2.043	1	0.573
DOPEY2	Dopey family member 2	9980	hs|21q22.12	2.118	-1.689	1	0.638
MCTP1	Multiple C2 domains, transmembrane 1	79772	hs|5q15	3.092	-1.179	0	0.749
CD84	CD84 molecule	8832	hs|1q23.3	3.645	-1.970	1	0.781
DCLK1	Doublecortin-like kinase 1	9201	hs|13q13.3	3.633	-1.286	2	0.804
CMPK2	Cytidine monophosphate (UMP-CMP) kinase 2, mitochondrial	129607	hs|2p25.2	2.748	-1.538	1	0.829
BHLHE41	Basic helix-loop-helix family, member e41	79365	hs|12p12.1	9.461	-1.129	2	0.895
ARHGAP42	Rho GTPase activating protein 42	143872	hs|11q22.1	2.075	-1.514	2	0.0000485*
SERTAD2	SERTA domain containing 2	9792	hs|2p14	2.183	-1.375	1	0.00549*
FAR2	Fatty acyl CoA reductase 2	55711	hs|12p11.22	2.113	-1.022	1	0.0136*

*, poor prgonosis in patients with low gene expression.

Table 3. Candidate *miR-532-3p* target genes in RCC

Gene Symbol	Gene Name	Entrez Gene ID	Cytoband	GEO expression data Fold-Change (Tumor/Normal)	miR-532-3p transfection in 786-O (Log$_2$ ratio)	Binding Sites Count	TCGA analysis for OS (high vs low expression: p value)
C1orf216	Chromosome 1 open reading frame 216	127703	hs|1p34.3	2.220	-1.493	1	5.69E-06
RRM2	Ribonucleotide reductase M2	6241	hs|2p25.1	4.814	-1.939	4	1.91E-05
AQP9	Aquaporin 9	366	hs|15q21.3	2.077	-1.455	1	2.03E-05
PLXDC1	Plexin domain containing 1	57125	hs|17q12	3.144	-1.534	2	0.00186
SLC6A1	Solute carrier family 6 (neurotransmitter transporter), member 1	6529	hs|3p25.3	2.527	-1.548	1	0.00285
CHST2	Carbohydrate (N-acetylglucosamine-6-O) sulfotransferase 2	9435	hs|3q24	2.232	-1.381	1	0.00288
PTP4A3	Protein tyrosine phosphatase type IVA, member 3	11156	hs|8q24.3	2.360	-1.542	1	0.00694
SERPING1	Serpin peptidase inhibitor, clade G (C1 inhibitor), member 1	710	hs|11q12.1	2.015	-1.244	1	0.0169
SLC7A11	Solute carrier family 7 (anionic amino acid transporter light chain, xc- system), member 11	23657	hs|4q28.3	2.678	-1.125	1	0.0234
CSF1	Colony stimulating factor 1 (macrophage)	1435	hs|1p13.3	2.021	-1.323	3	0.027
HCG27	HLA complex group 27 (non-protein coding)	253018	hs|6p21.33	2.421	-1.053	2	0.0447
CARD11	Caspase recruitment domain family, member 11	84433	hs|7p22.2	2.190	-1.698	1	0.0556
KIAA1462	KIAA1462	57608	hs|10p11.23	2.183	-1.551	1	0.0684
SCD	Stearoyl-CoA desaturase (delta-9-desaturase)	6319	hs|10q24.31	6.464	-2.610	1	0.129
ADAMTS2	ADAM metallopeptidase with thrombospondin type 1 motif, 2	9509	hs|5q35.3	2.863	-1.150	2	0.132
DOCK2	Dedicator of cytokinesis 2	1794	hs|5q35.1	5.262	-1.429	2	0.172
PGBD5	PiggyBac transposable element derived 5	79605	hs|1q42.13	3.517	-1.212	1	0.176
RUNX3	Runt-related transcription factor 3	864	hs|1p36.11	3.644	-1.263	2	0.213
MET	Met proto-oncogene	4233	hs|7q31.2	2.553	-1.684	1	0.224
TTYH3	Tweety family member 3	80727	hs|7p22.3	2.138	-1.423	1	0.247
DTX3L	Deltex 3-like (Drosophila)	151636	hs|3q21.1	2.253	-1.338	2	0.272
PSMB9	Proteasome (prosome, macropain) subunit, beta type, 9	5698	hs|6p21.32	3.722	-1.137	4	0.367
NCAPG2	Non-SMC condensin II complex, subunit G2	54892	hs|7q36.3	2.127	-1.127	1	0.385
MEF2C	Myocyte enhancer factor 2C	4208	hs|5q14.3	2.693	-1.276	1	0.472
PFKFB3	6-phosphofructo-2-kinase/fructose-2,6-biphosphatase 3	5209	hs|10p15.1	2.217	-1.285	1	0.507
RTP4	Receptor (chemosensory) transporter protein 4	64108	hs|3q27.3	3.204	-1.335	1	0.545
TRIM9	Tripartite motif containing 9	114088	hs|14q22.1	3.764	-2.307	3	0.552
TMEM92	Transmembrane protein 92	162461	hs|17q21.33	2.788	-2.151	4	0.635
RNF145	Ring finger protein 145	153830	hs|5q33.3	2.430	-1.203	1	0.751
RASSF2	Ras association (RalGDS/AF-6) domain family member 2	9770	hs|20p13	6.147	-2.224	3	0.911
BICD1	Bicaudal D homolog 1 (Drosophila)	636	hs|12p11.21	2.423	-1.079	1	0.955
KDR	Kinase insert domain receptor (a type III receptor tyrosine kinase)	3791	hs|4q12	2.040	-1.301	1	0.00000477*
ZBTB42	Zinc finger and BTB domain containing 42	100128927	hs|14q32.33	2.091	-2.218	3	0.000469*
DIRAS2	DIRAS family, GTP-binding RAS-like 2	54769	hs|9q22.2	6.202	-1.019	4	0.00119*

*, poor prgonosis in patiets with low gene expression.
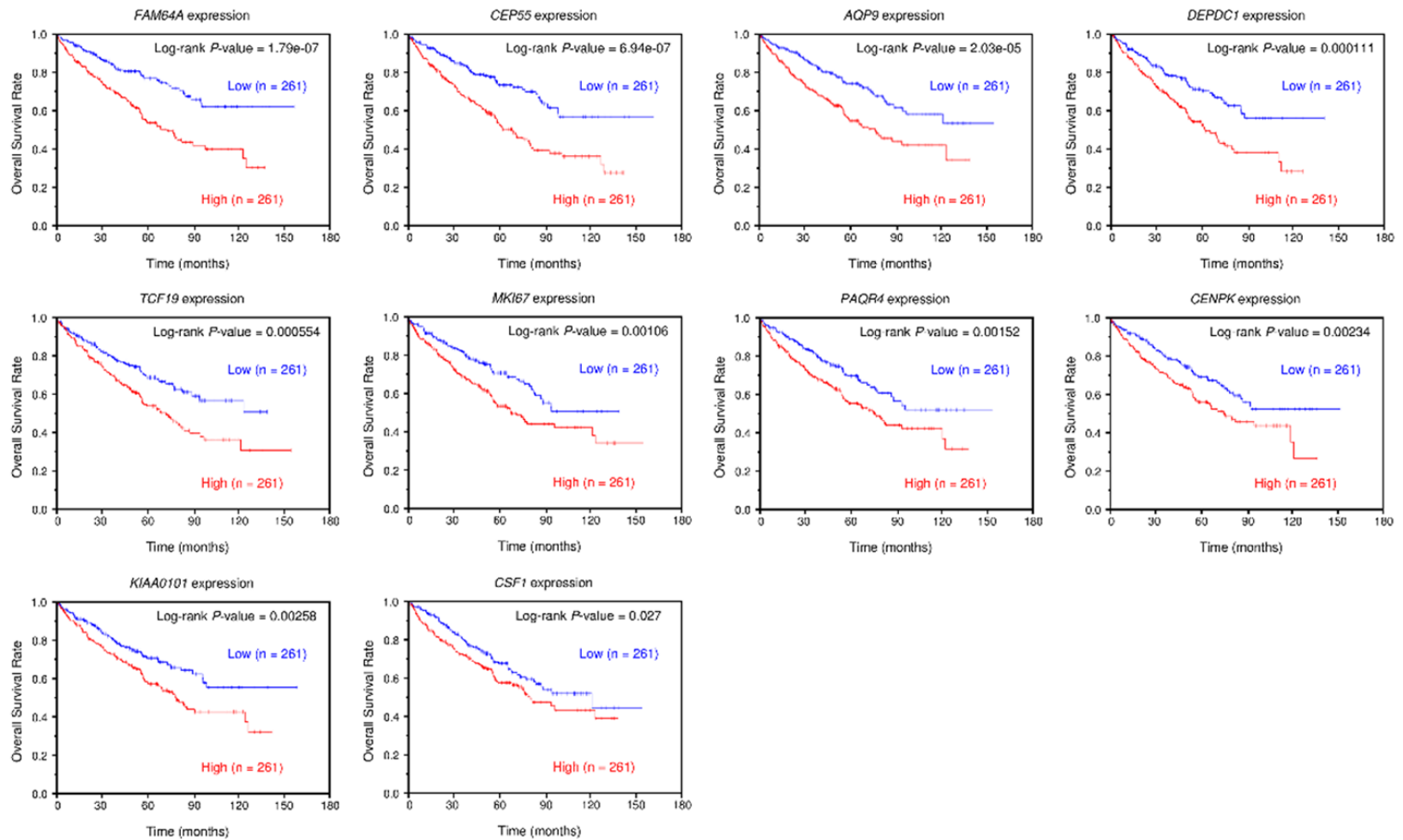
Figure 4. Kaplan-Meier analysis of candidate targets of *miR-532-5p* from TCGA database. Kaplan-Meier plots to compare overall survival rates of patients that had high (red lines) and low (blue lines) expression of 10 genes regulated by *miR-532-5p* (patients were divided in half).
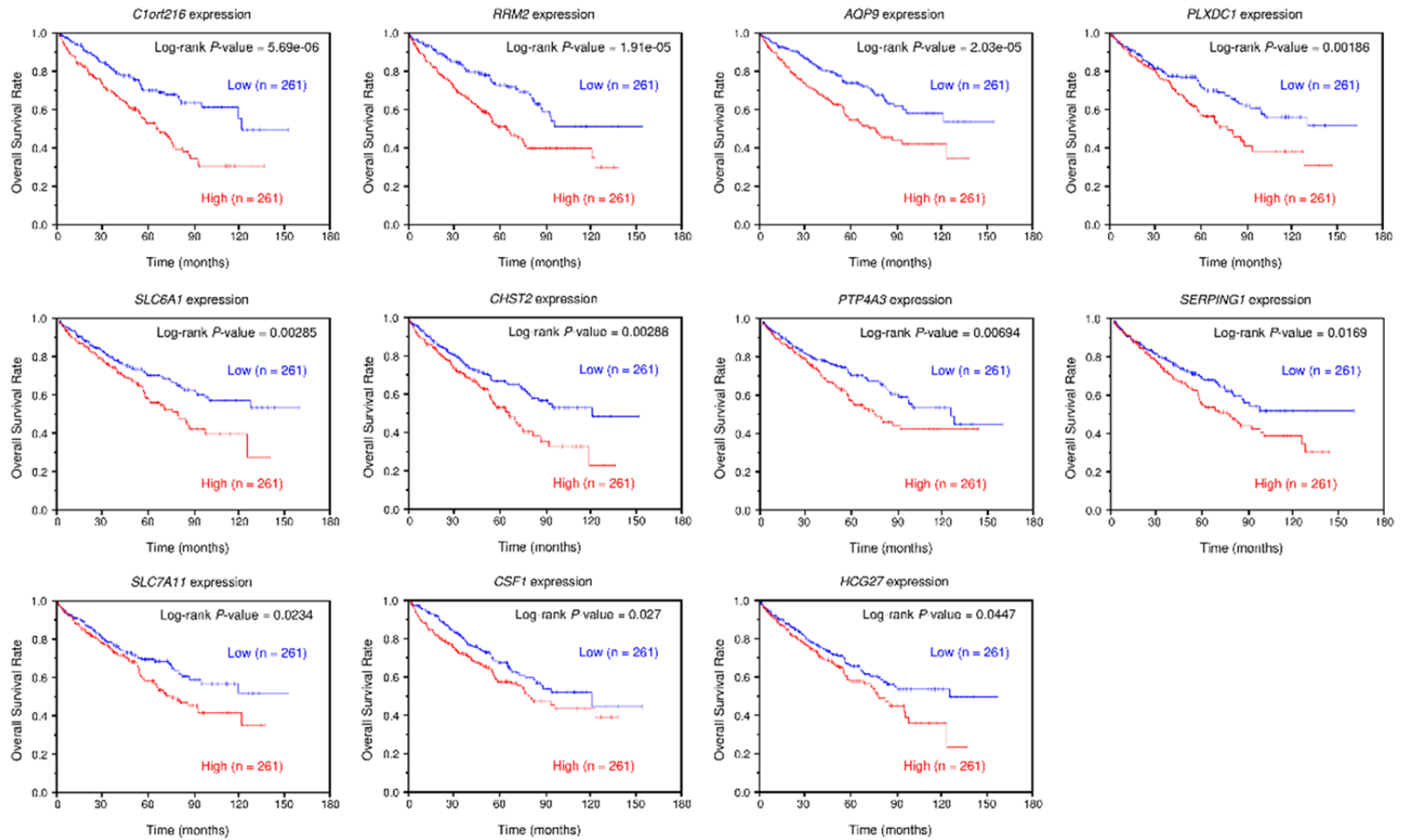
Figure 5. Kaplan-Meier analysis of candidate targets of *miR-532-3p* from TCGA database. Kaplan-Meier plots to compare overall survival rates of patients that had high (red lines) and low (blue lines) expression of 11 genes regulated by *miR-532-5p* (patients were divided in half).
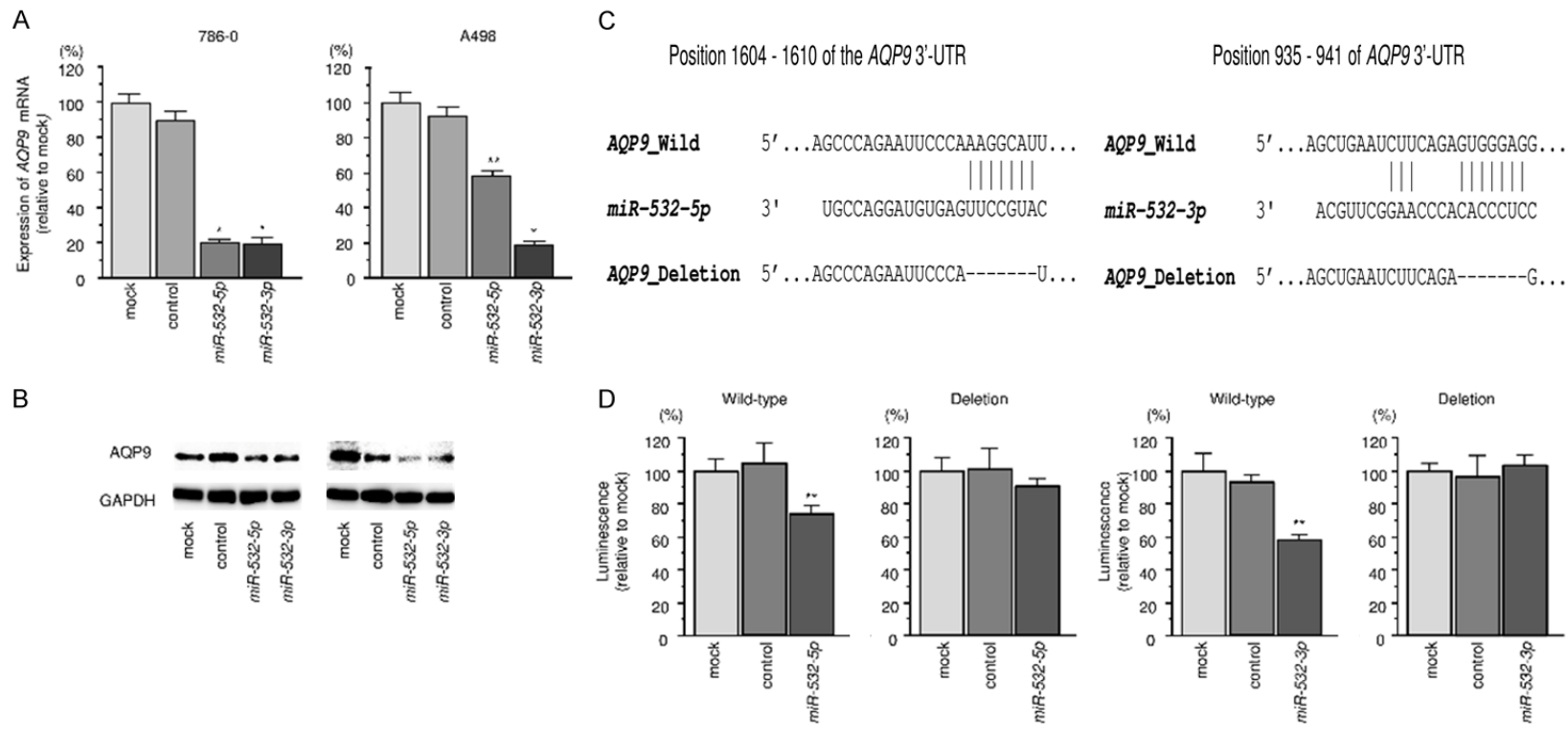
Figure 6. Direct regulation of *AQP9* expression by *miR-532-5p* and *miR-532-3p*. A. *AQP9* mRNA expression levels 48 h after transfection of 786-0 or A498 RCC cells with 10 nM *miR-532-5p* or *miR-532-3p*. *GAPDH* was used as an internal control. B. Protein expression of AQP9 72 h after transfection with *miR-532-5p* or *miR-532-3p*. GAPDH was used as a loading control. C. *miR-532-5p* and *miR-532-3p* binding sites in the *AQP9* mRNA 3'-UTR. D. Dual luciferase reporter assays with vectors encoding putative *miR-532-5p* and *miR-532-3p* target sites in the wild-type *AQP9* 3'-UTR and a 3'-UTR with the target sites deleted (Deletion). Normalized data were calculated as the ratio of *Renilla*/firefly luciferase activities. *$P < 0.0001$, **$P < 0.01$.
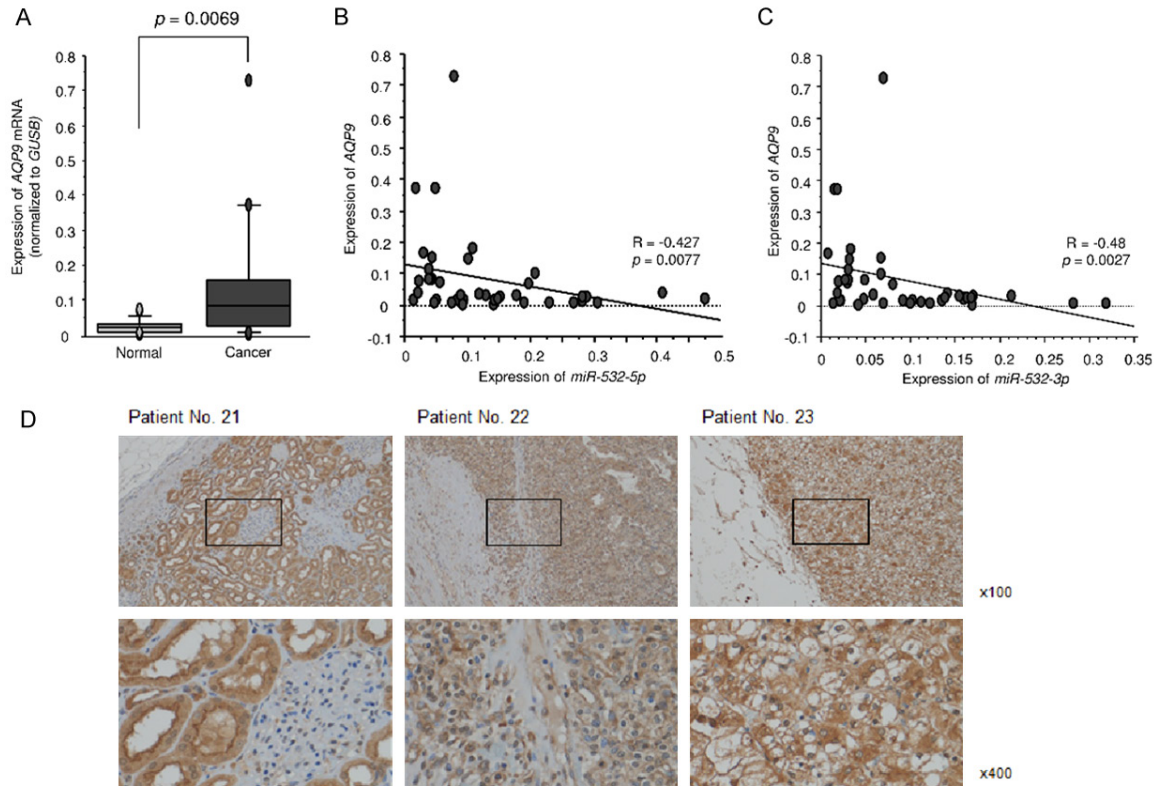
Figure 7. Expression of *AQP9* in clinical specimens. A. Expression levels of mRNA *AQP9* in RCC clinical specimens. *GUSB* was used as an internal control. B, C. Spearman's rank test showed a significant negative correlation between *AQP9* expression and *miR-532-5p* or *miR-532-3p* levels. D. Immunostaining showed that AQP9 levels were substantially higher in cancer lesions compared to normal tissues with the same staining intensity (100× and 400× magnification field).

Direct regulation of AQP9 expression by miR-532-5p and miR-52-3p

Levels of AQP9 mRNA and protein were significantly suppressed following transfection of 786-0 and A498 cells with *miR-532-5p* or *miR-532-3p* compared with mock-transfected cells or those transfected with miR-control (**Figure 6A**, **6B**).

The TargetScan Human database indicated the presence of binding sites for both *miR-532-5p* (position 1604-1610) and *miR-532-3p* (position 935-941) in the *AQP9* 3'-UTR. Thus, we performed luciferase reporter assays with a vector including these sequences to assess whether *miR-532-5p* and *miR-532-3p* directly regulated *AQP9* expression in a sequence-dependent manner. Cotransfection with *miR-532-5p* or *miR-532-3p* with vectors significantly suppressed luciferase activity in comparison with those in mock and miR-control transfectants (**Figure 6C**, **6D**).

Expression of AQP9 in clinical specimens

AQP9 mRNA expression levels were significantly upregulated in cancer tissues compared with that in adjacent noncancerous tissues ($P = 0.0069$) (**Figure 7A**). Spearman's rank test revealed a negative correlation between *AQP9* expression and that of the *miR-532-duplex* (5p; $P = 0.0077$, R = -0.427 and 3p; $P = 0.0027$, R = -0.48, respectively; **Figure 7B**, **7C**). Immunostaining for AQP9 in RCC clinical specimens indicated that AQP9 was strongly overexpressed in cancer lesions compared with adjacent noncancerous tissues at the same staining intensity (**Figure 7D**).

Relationship between pre-miR-532 and AQP9 in RCC pathogenesis and clinical outcome

In analyses of TCGA database, patients with high *AQP9* expression had significantly advanced tumor stage and pathological grade (**Figure 8A-C**). A multivariate Cox proportional
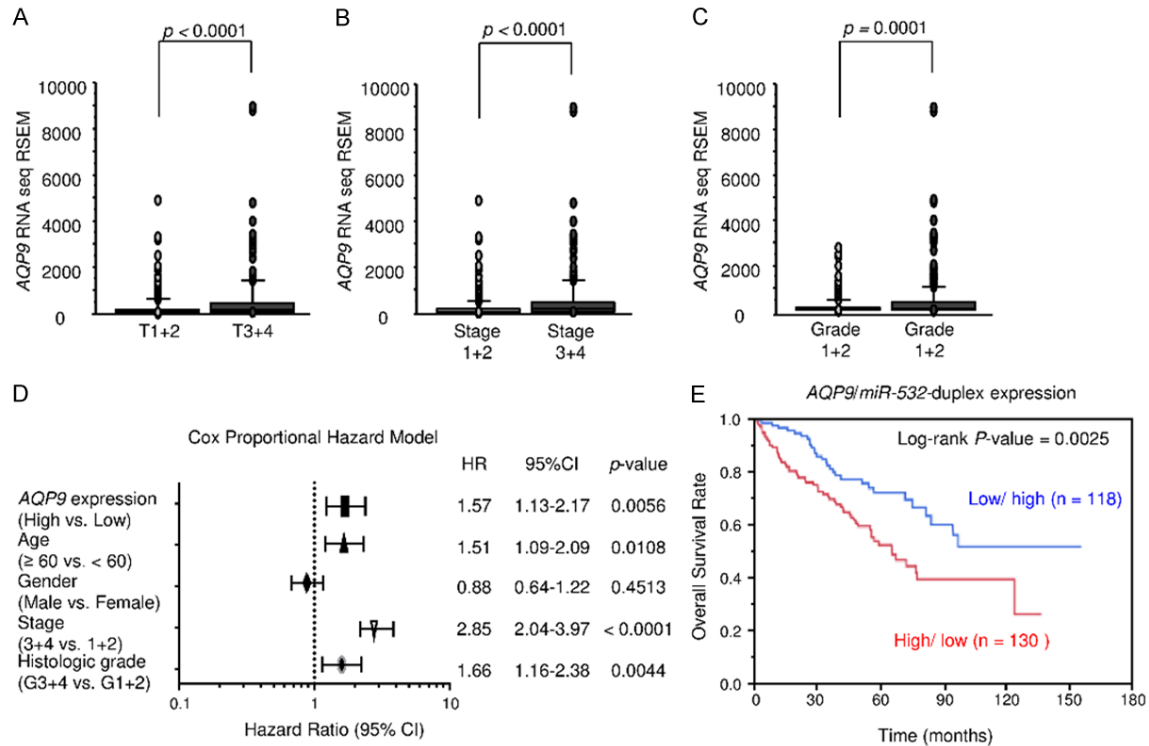
Figure 8. Clinical significance of *AQP9*. A-C. High *AQP9* expression levels were significantly associated with advanced tumor stage and pathological grade. D. Multivariate analysis for overall survival as a function of clinical parameters, including AQP9 expression. E. Kaplan-Meier plots to analyze overall survival showed that patients with high *AQP9* and low *miR-532-duplex* expression levels had significantly poorer prognosis compared with those that had low and high expression levels of *AQP9* and *miR-532-duplex*, respectively.

hazards model showed that high expression of *AQP9* was an independent predictive factor for overall survival (hazard ratio [HR]: 1.57, 95% confidence interval [CI]: 1.13-2.17, *P* = 0.0056) and was similar to well-known clinical prognostic factors such as age, tumor stage and grade (**Figure 8D**). A combined analysis of overall survival as related to *AQP9* and *miR-532-duplex* expression using the Kaplan-Meier method indicated that high *AQP9* and low *miR-532-duplex* expression levels were significantly associated with poor prognosis compared with low *AQP9* and high *miR-532-duplex* expression levels (*P* = 0.0025, **Figure 8E**).

Knockdown assay of AQP9 with siRNA

We confirmed that expression levels of both AQP9 mRNA and protein could be suppressed by si-*AQP9* transfection of RCC cells (**Figure 9A**, **9B**). Furthermore, *AQP9* silencing reduced migration and invasion activity of these cells (**Figure 9C-E**). A venn diagram of genes that showed significant changes in expression lev-

els following si-*AQP9* transfection and in RCC patient samples revealed that 64 genes were downregulated after transfection with si-*AQP9* and upregulated in RCC (**Figure 9F**; **Table 4**). In a KEGG analysis, we identified five pathways that included genes with differing expression that could be affected by altered *AQP9* expression.

Rescue studies by co-transfection of AQP9/ miR-532-duplex into A498 cells

We performed A*QP9* rescue studies in A498 cells to determine whether oncogenic pathways regulated by *AQP9/miR-532-duplex* are important for the development of RCC. *AQP9* and *miR-532-duplex* transfection restored AQP9 protein expression (**Figure 10A**, **10B**). Functional assays demonstrated that migration and invasion of RCC cells were significantly recovered by *AQP9* and *miR-532-duplex* transfection compared with cells with restored *miR-532-duplex* alone (**Figure 10C-E**).
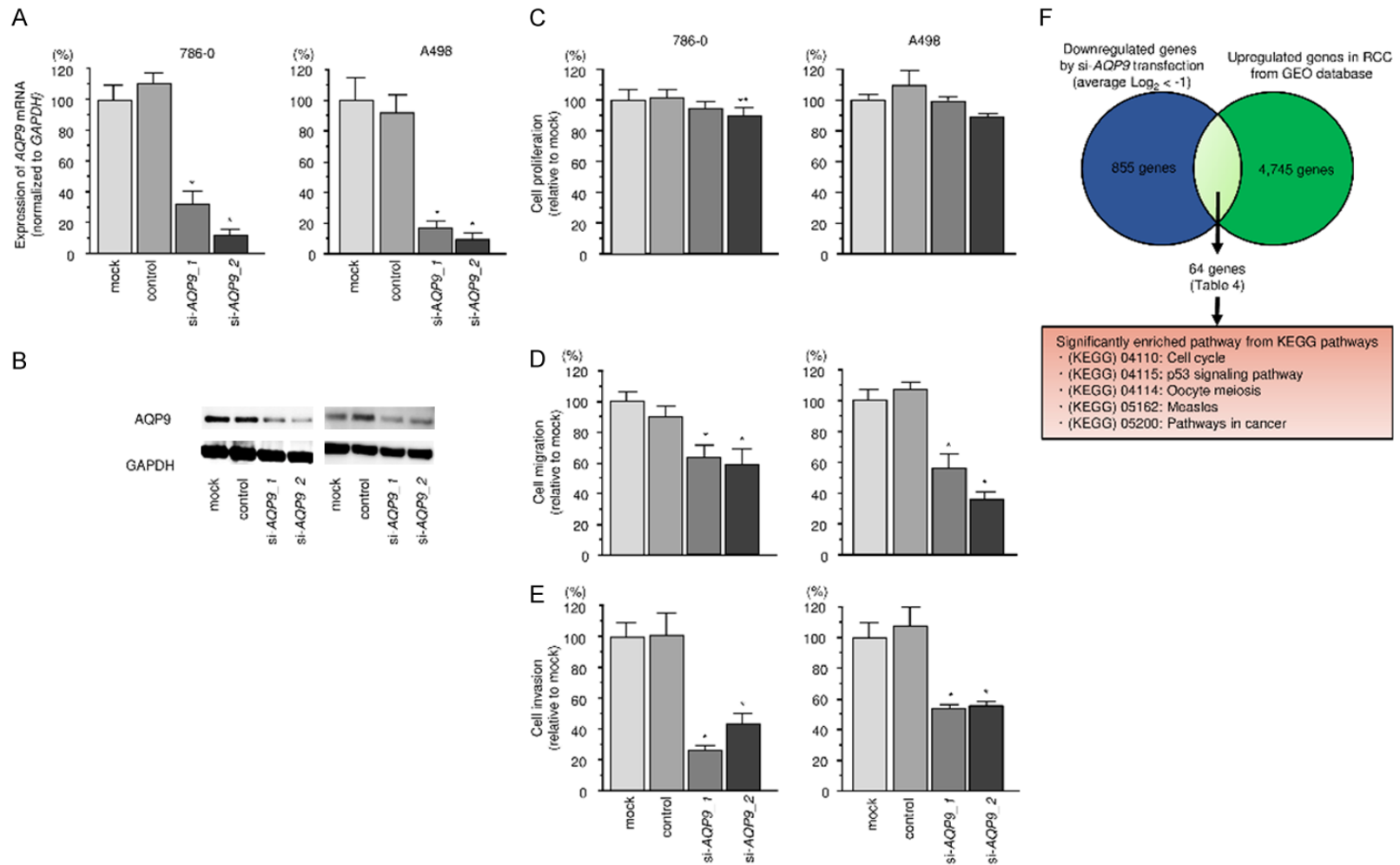
Figure 9. *AQP9* knockdown assay by siRNA. A, B. AQP9 mRNA and protein expression 72 h after transfection with si-*AQP9*_1 or si-*AQP9*_2 into RCC cell lines. *GUSB* and GAPDH were used as controls. C-E. Cell proliferation, migration and invasion activities. F. Venn diagram showing downregulated genes after transfection with si-*AQP9* and upregulated genes in RCC. KEGG analysis was used to identify enriched pathways. *$P < 0.0001$, **$P < 0.005$.

Table 4. Genes downstream of *AQP9* in RCC

Gene Symbol	Gene Name	Entrez Gene ID	Cytoband	Average si-AQP9_1 and 2 transfection in A498 (Log$_2$ ratio)	GEO expression data Fold-Change (Tumor/Normal)	TCGA analysis for OS (high vs low expression: *p* value)
TLR4	Toll-like receptor 4	7099	hs|9q33.1	-2.113	1.734	0.00171*
TIGIT	T cell immunoreceptor with Ig and ITIM domains	201633	hs|3q13.31	-2.074	3.185	0.0411
CALCRL	Calcitonin receptor-like	10203	hs|2q32.1	-2.025	1.826	5.31E-06*
PABPC4	Poly (A) binding protein, cytoplasmic 4 (inducible form)	8761	hs|1p34.3	-1.981	1.755	0.0000124
FOXO6	Forkhead box O6	100132074	hs|1p34.2	-1.928	1.746	no data
MX2	MX dynamin-like GTPase 2	4600	hs|21q22.3	-1.785	1.508	3.81E-08
DOCK9	Dedicator of cytokinesis 9	23348	hs|13q32.3	-1.745	1.614	1.1E-05*
SP140	SP140 nuclear body protein	11262	hs|2q37.1	-1.707	1.800	0.000889
CCNE2	Cyclin E2	9134	hs|8q22.1	-1.622	2.430	0.00664
AQP9	Aquaporin 9	366	hs|15q21.3	-1.596	2.077	0.0000203
S100A8	S100 calcium binding protein A8	6279	hs|1q21.3	-1.529	1.770	0.00999
RASA2	RAS p21 protein activator 2	5922	hs|3q23	-1.478	1.468	0.0275*
ELK1	ELK1, member of ETS oncogene family	2002	hs|Xp11.23	-1.433	1.514	0.0000286
MID1	Midline 1	4281	hs|Xp22.2	-1.432	1.515	0.284
OAS2	2'-5'-oligoadenylate synthetase 2, 69/71 kDa	4939	hs|12q24.13	-1.428	2.833	0.525
CHEK2	Checkpoint kinase 2	11200	hs|22q12.1	-1.407	1.947	2.67E-08
SLC15A3	Solute carrier family 15 (oligopeptide transporter), member 3	51296	hs|11q12.2	-1.381	4.754	0.213
EMILIN2	Elastin microfibril interfacer 2	84034	hs|18p11.31	-1.373	2.454	0.0345
ACTG2	Actin, gamma 2, smooth muscle, enteric	72	hs|2p13.1	-1.366	4.204	0.631
BIRC5	Baculoviral IAP repeat containing 5	332	hs|17q25.3	-1.355	2.729	2.93E-09
TIFA	TRAF-interacting protein with forkhead-associated domain	92610	hs|4q25	-1.354	1.782	0.507
CARD8	Caspase recruitment domain family, member 8	22900	hs|19q13.33	-1.293	1.650	0.854
SNHG1	Small nucleolar RNA host gene 1 (non-protein coding)	23642	hs|11q12.3	-1.273	2.163	0.000575
CDK1	Cyclin-dependent kinase 1	983	hs|10q21.2	-1.269	2.129	0.0000667
PLK1	Polo-like kinase 1	5347	hs|16p12.2	-1.238	2.643	3.59E-08
RPL28	Ribosomal protein L28	6158	hs|19q13.42	-1.235	1.424	0.00000308
BTNL9	Butyrophilin-like 9	153579	hs|5q35.3	-1.228	2.387	0.000973*
TBC1D10C	TBC1 domain family, member 10C	374403	hs|11q13.2	-1.223	3.069	0.0116
BDNF	Brain-derived neurotrophic factor	627	hs|11p14.1	-1.216	3.163	0.0591
GRIA4	Glutamate receptor, ionotropic, AMPA 4	2893	hs|11q22.3	-1.214	2.292	0.0372*
SFTA1P	Surfactant associated 1, pseudogene	207107	hs|10p14	-1.207	3.020	0.869
MIAT	Myocardial infarction associated transcript (non-protein coding)	440823	hs|22q12.1	-1.187	1.428	5.69E-08
SLC37A1	Solute carrier family 37 (glucose-6-phosphate transporter), member 1	54020	hs|21q22.3	-1.172	1.512	0.0821
RNF149	Ring finger protein 149	284996	hs|2q11.2	-1.170	2.161	0.118

TMEM180	Transmembrane protein 180	79847	hs|10q24.32	-1.167	2.287	No data
ABL2	ABL proto-oncogene 2, non-receptor tyrosine kinase	27	hs|1q25.2	-1.160	1.431	0.237
CXCL13	Chemokine (C-X-C motif) ligand 13	10563	hs|4q21.1	-1.160	11.383	0.00107
ERCC5	Excision repair cross-complementation group 5	2073	hs|13q33.1	-1.129	1.644	0.854
CDKN2A	Cyclin-dependent kinase inhibitor 2A	1029	hs|9p21.3	-1.127	3.422	0.0103
XAF1	XIAP associated factor 1	54739	hs|17p13.1	-1.121	2.349	0.0000172
ANKRD36BP2	Ankyrin repeat domain 36B pseudogene 2	645784	hs|2p11.2	-1.101	1.636	0.000000142
RDM1	RAD52 motif containing 1	201299	hs|17q12	-1.095	2.197	0.0145
PLK4	Polo-like kinase 4	10733	hs|4q28.2	-1.095	1.768	0.0266
TRIM9	Tripartite motif containing 9	114088	hs|14q22.1	-1.091	3.764	0.552
IFIT2	Interferon-induced protein with tetratricopeptide repeats 2	3433	hs|10q23.31	-1.081	1.655	0.869
TPR	Translocated promoter region, nuclear basket protein	7175	hs|1q31.1	-1.074	1.663	0.0124*
ZNF691	Zinc finger protein 691	51058	hs|1p34.2	-1.074	1.416	0.449
SFMBT2	Scm-like with four mbt domains 2	57713	hs|10p14	-1.067	2.189	0.00977*
SLC2A5	Solute carrier family 2 (facilitated glucose/fructose transporter), member 5	6518	hs|1p36.23	-1.060	1.787	0.863
HIST1H3H	Histone cluster 1, H3h	8357	hs|6p22.1	-1.053	3.446	0.516
MYO1G	Myosin IG	64005	hs|7p13	-1.045	2.669	0.0204
EPSTI1	Epithelial stromal interaction 1 (breast)	94240	hs|13q14.11	-1.043	1.556	0.337
LOXL3	Lysyl oxidase-like 3	84695	hs|2p13.1	-1.034	1.678	0.0012
NR5A2	Nuclear receptor subfamily 5, group A, member 2	2494	hs|1q32.1	-1.031	2.587	0.506
PRR3	Proline rich 3	80742	hs|6p21.33	-1.028	1.636	0.00115
DDX60	DEAD (Asp-Glu-Ala-Asp) box polypeptide 60	55601	hs|4q32.3	-1.018	1.460	0.000848*
C1RL	Complement component 1, r subcomponent-like	51279	hs|12p13.31	-1.018	1.579	0.000000173
TNFRSF4	Tumor necrosis factor receptor superfamily, member 4	7293	hs|1p36.33	-1.017	2.775	0.849
TET3	Tet methylcytosine dioxygenase 3	200424	hs|2p13.1	-1.013	1.664	0.0188
NEURL1B	Neuralized E3 ubiquitin protein ligase 1B	54492	hs|5q35.1	-1.008	2.907	0.0343*
LINGO1	Leucine rich repeat and Ig domain containing 1	84894	hs|15q24.3	-1.007	2.240	0.0344
TNFSF13B	Tumor necrosis factor (ligand) superfamily, member 13b	10673	hs|13q33.3	-1.007	4.786	0.00527
SQRDL	Sulfide quinone reductase-like (yeast)	58472	hs|15q21.1	-1.003	1.899	0.784
EVI2A	Ecotropic viral integration site 2A	2123	hs|17q11.2	-1.003	2.971	0.00737

*, poor prgonosis in patiets with low gene expression.
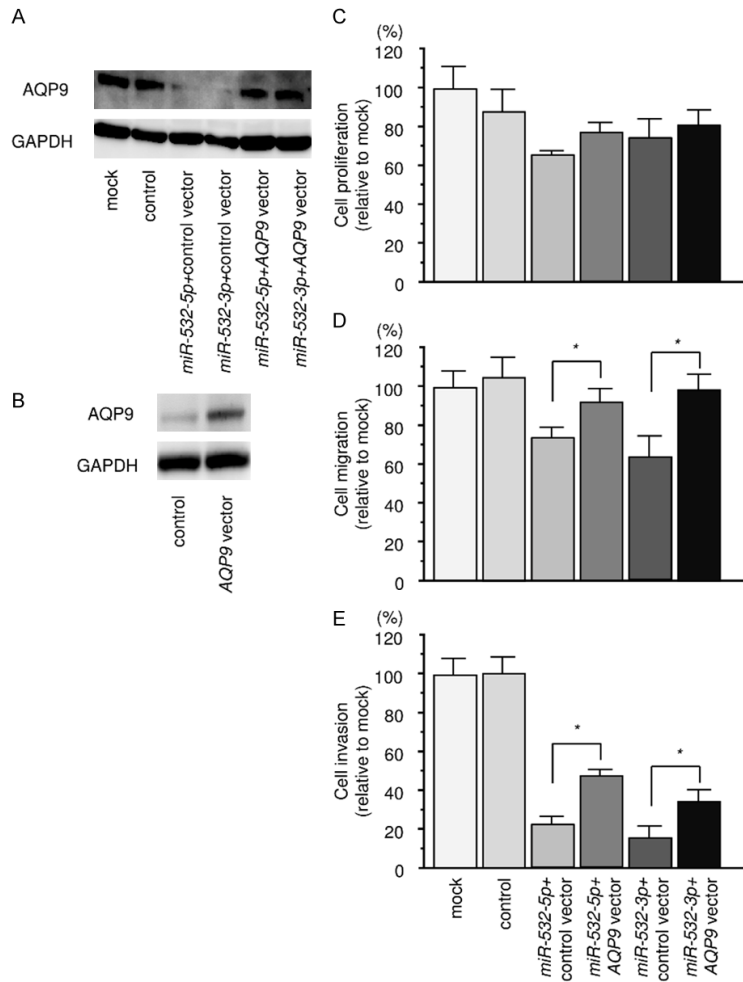
Figure 10. Effect of co-transfection of *AQP9/miR-532-duplex* into A498 cells. A, B. AQP9 protein expression was evaluated 72 h after reverse transfection with *miR-532-duplex* and 48 h after forward transfection with the *AQP9* vector. GAPDH was used as a loading control. C. Cell proliferation assay performed 72 h after reverse transfection with *miR-532-duplex* and 48 h after forward transfection with the *AQP9* vector. D. Cell migration assay performed 48 h after reverse transfection with *miR-532-duplex* and 24 h after forward transfection with the *AQP9* vector. E. Cell invasion assay performed 48 h after reverse transfection with *miR-532-duplex* and 24 h after forward transfection with *AQP9* vector. *$P < 0.0001$.

Discussion

In contrast to previous theories concerning miRNA biogenesis, we previously revealed that both pre-miRNA strands have functional roles in cancer development (e.g., *miR-144*, *miR-145*, *miR-455* [9, 10, 16]. In this study, we demonstrated that expression of both strands of pre-*miR-532* (*miR-532-5p* and *miR-532-3p*) was suppressed in RCC tissues and that both strands could act as tumor suppressors. Moreover, the oncogenic genes regulated by pre-*miR-532* contributed to RCC pathogenesis. Interestingly, previous studies showed that

miR-532 has both cancer-promoting and suppressive effects, depending on the type of cancer. For instance, *miR-532-5p* expression is upregulated in gastric cancer cells and this increased expression was related to an aggressive cancer phenotype [17].

Meanwhile, *miR-532-5p* expression is downregulated in epithelial ovarian cancer (EOC), in which it functions as a tumor suppressive miRNA that directly targets *TWIST1* [18]. Tumor-suppressive functions for *miR-532-5p* were also reported for other cancer types [19].

In hepatocellular carcinoma (HCC), *miR-532-3p* (passenger strand) has a tumor-suppressive function by directly regulating the expression of the oncogenic kinesin family member C1 (*KIFC1*) and the *miR-532-3p/KIFC1* axis promoted epithelial to mesenchymal transition (EMT) and HCC metastasis [20]. For RCC, a previous study reported that *miR-532-5p* expression is downregulated and it functions as a tumor suppressor [21]. The transcription factor ETS1 directly binds the promoter region of pre-*miR-532* and negatively controls expression of *miR-532-5p* in RCC cells [21]. The above results showed that aberrant expression (up- or down-regulation) of *miR-532-5p* and *miR-532-3p* is closely associated with cancer pathogenesis. Notably, the two strands of pre-*miR-532* have opposite functions depending on the cancer type. Thus, elucidation of molecular mechanisms that regulate the expression of pre-*miR-532* is an important issue in cancer research.

For RCC, another area of interest is clarification of which RNA networks are controlled by strands of pre-*miR-532*. Using our search strategy to identify miRNA targets, in RCC cells we identified 36 and 34 genes as putative onco-

genic targets of *miR-532-5p* and *miR-532-3p*, respectively. Among these targets, high expression of 19 genes was closely associated with worse prognosis of RCC patients. Analysis of these genes will contribute to a better understanding of the molecular pathology of RCC.

Here we focused on aquaporin 9 (*AQP9*) because this gene was a putative target for both *miR-532-5p* and *miR-532-3p* in RCC cells and its expression was significantly associated with RCC pathogenesis, although its functional significance in RCC is poorly understood. Aquaporin genes (AQPs) encode a family of membrane-spanning water channels, of which 15 are known for mammals [22]. Previous studies showed that some AQPs have aberrant expression in cancer cells that is associated with cancer pathogenesis [23, 24]. AQP9 is permeable to small molecules including water, urea, glycerol, arsenite and H_2O_2, and plays a role in maintaining cellular water homeostasis and energy balance [25]. Previous studies detected overexpression of AQP9 in several cancers such as brain tumor, ovarian cancer and prostate cancer [26-28]. In astrocytoma cells, aberrant AQP9 expression induced AKT activation and decreased E-cadherin expression [29]. Meanwhile, overexpression of AQP9 induced cell cycle arrest and enhanced chemo-sensitivity to 5-fluorouracil in colorectal cancer [30]. The results of these studies suggest that AQP9 can act as an oncogene and thus could be a promising therapeutic target in human cancers.

Our functional assays showed that *AQP9* knockdown inhibited cancer cell migration and invasion, and *AQP9* overexpression promoted cancer cell aggressiveness in RCC. Aberrant expression of *AQP9* was also detected in RCC clinical specimens. We further investigated the expression of *AQP9*-mediated genes that function downstream of *AQP9* in RCC cells. Our data showed that several cell cycle-related genes (e.g., *CCNE2*, *CHEK2*, *PLK1*, *CDKN2A* and *CDK1*) were affected by aberrant *AQP9* expression. Expression of these cell cycle-related genes was closely associated with RCC patient prognosis. Our data suggested that aberrant expression of *AQP9* enhanced RCC oncogenesis and affected several oncogenic genes in RCC cells.

In conclusion, our results showed that expression of both strands of the pre-*miR-532-duplex* (*miR-532-5p* and *miR-532-3p*) was significantly downregulated in RCC clinical specimens and thus the *miR-532-duplex* could act as an antitumour miRNA in RCC. The expression of 19 genes was closely associated with RCC pathogenesis and the expression of these genes was controlled by the pre-*miR-532*-duplex. Among these targets, *AQP9* expression was directly regulated by both *miR-532-5p* and *miR-532-3p* in RCC cells. Aberrant expression of *AQP9* enhanced cancer aggressiveness, suggesting that *AQP9* could be a promising therapeutic target for RCC. Our approach based on antitumor miRNAs could contribute to the development of new diagnostic markers and therapeutic strategies for RCC.

Acknowledgements

Disclosure of conflict of interest

None.

Address correspondence to: Dr. Naohiko Seki, Department of Functional Genomics, Chiba University Graduate School of Medicine, 1-8-1 Inohana Chuo-ku, Chiba 260-8670, Japan. Tel: +81-43-226-2971; Fax: +81-43-227-3442; E-mail: naoseki@faculty.chiba-u.jp

References

[1] Capitanio U and Montorsi F. Renal cancer. Lancet 2016; 387: 894-906.

[2] Pierorazio PM, Johnson MH, Patel HD, Sozio SM, Sharma R, Iyoha E, Bass EB and Allaf ME. Management of renal masses and localized renal cancer: systematic review and meta-analysis. J Urol 2016; 196: 989-999.

[3] Figlin R, Sternberg C and Wood CG. Novel agents and approaches for advanced renal cell carcinoma. J Urol 2012; 188: 707-715.

[4] Bartel DP. MicroRNAs: target recognition and regulatory functions. Cell 2009; 136: 215-233.

[5] Goto Y, Kurozumi A, Nohata N, Kojima S, Matsushita R, Yoshino H, Yamazaki K, Ishida Y, Ichikawa T, Naya Y and Seki N. The microRNA signature of patients with sunitinib failure:

regulation of UHRF1 pathways by microR-NA-101 in renal cell carcinoma. Oncotarget 2016; 7: 59070-59086.

[6] Arai T, Okato A, Kojima S, Idichi T, Koshizuka K, Kurozumi A, Kato M, Yamazaki K, Ishida Y, Naya Y, Ichikawa T and Seki N. Regulation of spindle and kinetochore-associated protein 1 by antitumor miR-10a-5p in renal cell carcinoma. Cancer Sci 2017; 108: 2088-2101.

[7] Kurozumi A, Kato M, Goto Y, Matsushita R, Nishikawa R, Okato A, Fukumoto I, Ichikawa T and Seki N. Regulation of the collagen cross-linking enzymes LOXL2 and PLOD2 by tumor-suppressive microRNA-26a/b in renal cell carcinoma. Int J Oncol 2016; 48: 1837-1846.

[8] Yamada Y, Arai T, Sugawara S, Okato A, Kato M, Kojima S, Yamazaki K, Naya Y, Ichikawa T and Seki N. Impact of novel oncogenic pathways regulated by antitumor miR-451a in renal cell carcinoma. Cancer Sci 2018; 109: 1239-1253.

[9] Yamada Y, Arai T, Kojima S, Sugawara S, Kato M, Okato A, Yamazaki K, Naya Y, Ichikawa T and Seki N. Anti-tumor roles of both strands of the miR-455 duplex: their targets SKA1 and SKA3 are involved in the pathogenesis of renal cell carcinoma. Oncotarget 2018; 9: 26638-26658.

[10] Yamada Y, Arai T, Kojima S, Sugawara S, Kato M, Okato A, Yamazaki K, Naya Y, Ichikawa T and Seki N. Regulation of antitumor miR-144-5p targets oncogenes: direct regulation of syndecan-3 and its clinical significance. Cancer Sci 2018; 109: 2919-2936.

[11] Mah SM, Buske C, Humphries RK and Kuchenbauer F. miRNA*: a passenger stranded in RNA-induced silencing complex? Crit Rev Eukaryot Gene Expr 2010; 20: 141-148.

[12] Yamada Y, Sugawara S, Arai T, Kojima S, Kato M, Okato A, Yamazaki K, Naya Y, Ichikawa T and Seki N. Molecular pathogenesis of renal cell carcinoma: impact of the anti-tumor miR-29 family on gene regulation. Int J Urol 2018; 25: 953-965.

[13] J A. OncoLnc: linking TCGA survival data to mRNAs, miRNAs, and lncRNAs. PeerJ Computer Science 2016; 2: e67.

[14] Gao J, Aksoy BA, Dogrusoz U, Dresdner G, Gross B, Sumer SO, Sun Y, Jacobsen A, Sinha R, Larsson E, Cerami E, Sander C and Schultz N. Integrative analysis of complex cancer genomics and clinical profiles using the cBioPortal. Sci Signal 2013; 6: pl1.

[15] Cerami E, Gao J, Dogrusoz U, Gross BE, Sumer SO, Aksoy BA, Jacobsen A, Byrne CJ, Heuer ML, Larsson E, Antipin Y, Reva B, Goldberg AP, Sander C and Schultz N. The cBio cancer genomics portal: an open platform for exploring

multidimensional cancer genomics data. Cancer Discov 2012; 2: 401-404.

[16] Goto Y, Kurozumi A, Arai T, Nohata N, Kojima S, Okato A, Kato M, Yamazaki K, Ishida Y, Naya Y, Ichikawa T and Seki N. Impact of novel miR-145-3p regulatory networks on survival in patients with castration-resistant prostate cancer. Br J Cancer 2017; 117: 409-420.

[17] Hu S, Zheng Q, Wu H, Wang C, Liu T and Zhou W. miR-532 promoted gastric cancer migration and invasion by targeting NKD1. Life Sci 2017; 177: 15-19.

[18] Wei H, Tang QL, Zhang K, Sun JJ and Ding RF. miR-532-5p is a prognostic marker and suppresses cells proliferation and invasion by targeting TWIST1 in epithelial ovarian cancer. Eur Rev Med Pharmacol Sci 2018; 22: 5842-5850.

[19] Song Y, Zhao Y, Ding X and Wang X. microR-NA-532 suppresses the PI3K/Akt signaling pathway to inhibit colorectal cancer progression by directly targeting IGF-1R. Am J Cancer Res 2018; 8: 435-449.

[20] Han J, Wang F, Lan Y, Wang J, Nie C, Liang Y, Song R, Zheng T, Pan S, Pei T, Xie C, Yang G, Liu X, Zhu M, Wang Y, Liu Y, Meng F, Cui Y, Zhang B, Liu Y, Meng X, Zhang J and Liu L. KIFC1 regulated by miR-532-3p promotes epithelial-to-mesenchymal transition and metastasis of hepatocellular carcinoma via gankyrin/AKT signaling. Oncogene 2019; 38: 406-420.

[21] Zhai W, Ma J, Zhu R, Xu C, Zhang J, Chen Y, Chen Z, Gong D, Zheng J, Chen C, Li S, Li B, Huang Y, Xue W and Zheng J. MiR-532-5p suppresses renal cancer cell proliferation by disrupting the ETS1-mediated positive feedback loop with the KRAS-NAP1L1/P-ERK axis. Br J Cancer 2018; 119: 591-604.

[22] De Ieso ML and Yool AJ. Mechanisms of aquaporin-facilitated cancer invasion and metastasis. Front Chem 2018; 6: 135.

[23] Nico B and Ribatti D. Aquaporins in tumor growth and angiogenesis. Cancer Lett 2010; 294: 135-138.

[24] Papadopoulos MC and Saadoun S. Key roles of aquaporins in tumor biology. Biochim Biophys Acta 2015; 1848: 2576-2583.

[25] Yang JH, Yan CX, Chen XJ and Zhu YS. Expression of aquaglyceroporins in epithelial ovarian tumours and their clinical significance. J Int Med Res 2011; 39: 702-711.

[26] Fossdal G, Vik-Mo EO, Sandberg C, Varghese M, Kaarbo M, Telmo E, Langmoen IA and Murrell W. Aqp 9 and brain tumour stem cells. ScientificWorldJournal 2012; 2012: 915176.

[27] Yang JH, Yu YQ and Yan CX. Localisation and expression of aquaporin subtypes in epithelial ovarian tumours. Histol Histopathol 2011; 26: 1197-1205.

[28] Chen Q, Zhu L, Zheng B, Wang J, Song X, Zheng W, Wang L, Yang D and Wang J. Effect of AQP9 expression in androgen-independent prostate cancer cell PC3. Int J Mol Sci 2016; 17.

[29] Lv Y, Huang Q, Dai W, Jie Y, Yu G, Fan X, Wu A and Miao Q. AQP9 promotes astrocytoma cell invasion and motility via the AKT pathway. Oncol Lett 2018; 16: 6059-6064.

[30] Huang D, Feng X, Liu Y, Deng Y, Chen H, Chen D, Fang L, Cai Y, Liu H, Wang L, Wang J and Yang Z. AQP9-induced cell cycle arrest is associated with RAS activation and improves chemotherapy treatment efficacy in colorectal cancer. Cell Death Dis 2017; 8: e2894.